HHS Public Access

Author manuscript

Mol Carcinog. Author manuscript; available in PMC 2021 February 16.

Published in final edited form as:

Mol Carcinog. 2017 February ; 56(2): 489–498. doi:10.1002/mc.22511.

Loss of Tyrosine Phosphorylation at Y406 Abrogates the Tumor Suppressor Functions of the Thyroid Hormone Receptor β

Jeong Won Park, **Li Zhao**, **Mark C. Willingham**, **Sheue-yann Cheng***

Laboratory of Molecular Biology, Center for Cancer Research, National Cancer Institute, National Institutes of Health, Bethesda, Maryland

Abstract

We have recently identified that phosphorylation at tyrosine (Y)406 is critical for the tumor suppressor functions of the thyroid hormone receptor β1 (TRβ) in a breast cancer line. However, still unclear is whether the critical tumor suppressor role of phosphorylated Y406 of TRβ is limited to only breast cancer cells or could be extended to other cell types. In the present studies, we addressed this question by stably expressing TRβ, a mutated TRβ oncogene (PV), or a TRβ mutated at Y406 (TRβY406F) in rat PCCL3 thyroid follicular cells and evaluated their tumor characteristics in athymic mice with elevated thyroid stimulating hormone. PCCL3 cells stably expressing PV (PCCL3-PV), TRβY406F (PCCL3-TRβY406F), vector only (PCCL3-Neo) developed tumors with sizes in the rank order of TRβY406F>PV = Neo, whereas PCCL3 cells expressing TRβ (PCCL3-TRβ) barely developed tumors. As evidenced by markedly elevated Ki67, cyclin D1, and p-Rb protein abundance, proliferative activity was high in PV and TRβY406F tumors, but low in TRβ tumors. These results indicate that TRβ acted as a tumor suppressor in PCCL3 cells, whereas TRβY406F and PV had lost tumor suppressor activity. Interestingly, TRβY406F tumors had very low necrotic areas with decreased TNFα-NFκB signaling to lower apoptotic activity. In contrast, PV tumors had prominent large necrotic areas, with no apparent changes in TNFα-NFκB signaling, indicating distinct oncogenic activities of mutant PV and TRβY406F. Thus, the present studies uncovered a novel mechanism by which TRβ could function as a tumor suppressor through modulation of the TNFα-NFκB signaling.

Keywords

thyroid cancer; thyroid hormone receptor β mutant; phosphorylation of thyroid hormone receptor β1; tumor suppressor; xenograft models

INTRODUCTION

Thyroid hormone receptor β1 (TRβ) is a ligand-dependent transcription factor critical in growth, development, and differentiation. Since the cloning of the *THRB* gene in 1986 [1], studies of TRβ functions have been focused on its role in mediating the normal biological activities of the thyroid hormone T3. Recently, the idea that TRβ can function as a tumor

*Correspondence to: Laboratory of Molecular Biology, National Cancer Institute, 37 Convent Dr, Room 5128, Bethesda, MD 20892-6264.

suppressor in cancer development has gained increasing attention. Early studies indicated that truncations and/or deletions of chromosome 3p where the *THRB* gene is located are closely associated with human malignancies including lung, melanoma, breast, head and neck, renal cell, uterine cervical, ovarian, and testicular tumors [2–5]. Moreover, decreased expression resulting from the silencing of the *THRB* gene by promoter hypermethylation has been found in human cancer including breast, lung, and thyroid carcinoma [6–9].

In addition to these positive association studies, recent work has proposed molecular mechanisms by which TRβ can function as a tumor suppressor. Cell-based studies have shown that over-expressed TRβ reduces tumor growth and causes partial mesenchymal-to-epithelial cell transition (β-catenin, vimentin, and cytokeratin 8/18) in hepatocarcinoma and breast cancer cells [10]. In neuroblastoma cells, the over-expressed TRβ inhibits the transcriptional response of the Ras/mitogen-activated protein kinase/ribosomal-S6 pathway, thereby suppressing growth [11]. Similarly, over-expressed TRβ was also shown to inhibit AKT-mTOR-p70S6K pathways in human follicular thyroid cancer cells [12]. In human breast cancer cells, TRβ suppresses estrogen-dependent tumor growth by down-regulation of JAK-STAT-cyclin D pathways [13]. An additional mechanism by which TRβ could function as a tumor suppressor was recently uncovered [14]. TRβ up-regulates the expression of nuclear receptor corepressor 1 (NCOR1), which mediates the suppression of invasion, tumor growth, and metastasis in human hepatocarcinomas and more aggressive breast tumors [14].

We have previously identified a cSrc phosphorylation site on Y406 of TRβ [15]. Such phosphorylation on Y406 signals T3-induced degradation, thereby markedly attenuating cSrc signaling to suppress cell proliferation and invasiveness in breast cancer cells. When TRβY406 is mutated to 406F, no T3-induced degradation occurs, resulting in constitutive activation of cSrc signaling to promote oncogenesis [15]. However, it is not clear whether this cSrc-dependent tumor suppressor function of TRβ operates uniquely in breast cancer cells or could be extended to other cell types.

In the present studies, we stably expressed TRβY406F and TRβ in PCCL3 thyroid cells and assessed the effect of the loss of cSrc phosphorylation on the tumor suppressor function of TRβ. We also compared the oncogenic effect of a TRβ C-terminal frame-shift mutant PV in PCCL3 cells to that of TRβY406F. PV has been shown to be an oncogene in mouse models and in cultured cells [16–18]. We found that loss of the cSrc phosphorylation site on Y406 abrogated the tumor suppressor function of TRβ, thereby functioning as an oncogene in thyroid PCCL3 cells as it did in breast cancer cells. In addition, we uncovered that TRβY406F, but not PV, acted to attenuate the TNFα-IκBα-NFκB signaling, thereby decreasing necrotic activity and increasing tumor growth. Thus the present studies uncovered a novel mechanism by which TRβ could function as a tumor suppressor through modulation of TNFα-IκBα-NFκB pathway.

MATERIALS AND METHODS

Cell Lines

The PCCL3 cells were a generous gift from Professor R. Di Lauro (Napoli, Italy). Establishment of PCCL3 cells stably expressing human TRβ (PCCL3-TRβ cells), PV

(PCCL3-PV cells), TRβY406F (PCCL3-TRβY406F cells), or the control selectable marker Neo gene (Neo cells) was carried out similarly as described previously for PCCL3 cells [18]. Briefly, PCCL3 cells were transfected with the expression plasmid containing cDNA encoding Flag-hemagglutinin-TRβ (pcDNA3.1-FHTR-β), Flag-hemagglutinin-PV (pcDNA3.1-FH-PV), Flag-hemagglutinin-TRβY406F (pcDNA3.1-FH-TRβY406F), or the empty vector containing only the cDNA for the selector marker, the Neo gene. After transfection, cells were selected with 200 mg/ml G418 (Invitrogen, Carlsbad, CA) for 2 wk. G418-resistant colonies expressing TRβ and mutants (PV and TRβ1Y406F) were expanded for subsequent experiments. The expression of TRβ and mutant protein was verified by Western blot analysis using anti-TRβ antibodies (Rockland, Limerick, PA, cat. 600–401-A96).

Reporter Assays

PCCL3-parental and stably expressing cells (PCCL3-TRβ, PCCL3-PV, and PCCL3-TRβY406F) were seeded at a density of 5×10^5 in six-well culture plates and preincubated for 24 h with Td medium. Cells were transfected using Lipofectamine2000 (Invitrogen) using the protocol of the manufacturer. Briefly, 0.5 μg/well plasmid (pcDNA3.1-FH-TRβ or pcDNA3.1-FH-PV for PCCL3-parental cells) and 0.2 μg/well reporter plasmids (Pal-luc) were incubated with Lipofectamine2000 at room temperature for 20 min and then added to cells cultured in 1 ml OptiMEM. After a 3-h incubation, the medium was replaced by fresh 10% Td-fetal bovine serum with or without T3 (100 nM). Cells were lysed 24 h later with Luciferase Cell Culture Lysis 5X Reagent (Promega, Madison, WI), and luciferase activity was measured using Victor 3 (PerkinElmer Life and Analytical Sciences, Waltham, MA). Luciferase values were standardized to the ratio of activity to protein concentration.

In Vivo Mouse Xenograft Study

The protocols for the use and care of the animals in the present studies were approved by the National Cancer Institute Animal Care and Use Committee. Six-week-old female athymic NCr-nu/nu mice were obtained from the NCI-Frederick animal facility. The control PCCL3 cells (Neo) and PCCL3-TRβ or PCCL3-mutants (PV and Y406F) (5×10^6 cells) in 200 μl suspension mixed with Matrigel Basement Membrane Matrix (BD, Biosciences, San Jose, CA) were inoculated subcutaneously into the right flank of mice, similarly as previously described [18]. The mice were fed an iodine-deficient diet supplemented with 0.15% PTU (cat. no. TD.95125, Harlan Laboratories, Inc., Indianapolis, IN) beginning at 1 wk before cell injection and continued on the PTU diet until reaching near 2 cm in diameter, at which time the tumors were isolated for analyses. The tumor size was measured with calipers weekly until it reached ~2 cm in diameter. The tumor volume was calculated as $L \times W \times H \times 0.5236$.

Histopathologic Analysis

Xenograft tumors were dissected and fixed in 10% neutral-buffered formalin (Sigma–Aldrich, St. Louis, MO) and subsequently embedded in paraffin. Five-micrometer-thick sections were prepared and stained with hematoxylin and eosin (H&E). Immunohistochemistry was performed on formalin-fixed paraffin tumor sections, as previously described [19]. Primary antibodies used were anti-Ki-67 antibody (dilution

1:300; Thermo Scientific, Cambridge, MA) and anti-TNFα antibodies (dilution 1:100; Santa Cruz Biotechnology, Dallas, TX). Staining was developed with diaminobenzidine (DAB) using the DAB substrate kit for peroxidase (Vector Laboratories, Burlingame, CA). For quantitative analysis Ki-67 or TNFα positive cells were counted by using NIH Image J software version 1.47 (Wayne Rasband, National Institutes of Health, Bethesda, MD).

Western Blot

The western blot analysis was carried out as described by Park et al. [18]. The protein sample (20 μg) was loaded and separated by SDS–PAGE. After electrophoresis, the protein was electrotransferred to a poly vinylidene difluoride membrane (Immobilon-P; Millipore Corp., Billeria, MA). The antibodies phosphorylated Src (Y416, 1:500), total Src (1:1000), p-Rb (S780, 1:500 dilution), total Rb (1:1,000 dilution), p-IkBα (S32/36, 1:500 dilution), total IkBα (1:1,000 dilution), caspase 8 (1:1,000 dilution), and GAPDH (1:1,000 dilution) were purchased from Cell Signaling Technology (Denver, MA). Antibodies for VEGF (1:200 dilution) and TNFα (1:200 dilution) were purchased from Santa Cruz Biotechnology. Antibody for cyclin D1 (1:500 dilution) and TRβ (1:500) were purchased from Neomarkers (Thermo Scientific, Cambridge, MA) and Rockland, respectively. The blots were stripped with Re-Blot Plus (Millpore, Billeria, MA) and reprobed with rabbit polyclonal antibodies to GAPDH. Band intensities were quantified by using NIH IMAGE software (Image J 1.47).

Statistical Analysis

All data are expressed as mean ± standard error of the mean (SEM). Significant differences between groups were calculated using Student's *t*-test with the use of GraphPad Prism 6 (GraphPad Software, Inc., San Diego, CA). A P-value <0.05 is considered statistically significant.

RESULTS

Loss of the cSrc Phosphorylation Site at Y406 Abrogates the Tumor Suppressor Functions of TRβ by Propelling Tumor Cell Proliferation

Previously we have shown that mutation of tyrosine at amino acid 406 of TRβ1 to phenylalanine (designated as TRβY406F) leads to the loss of tumor suppressor functions of TRβ1 in breast cancer MDA cells [15]. Consequently, it functions as an oncogene. To understand whether the oncogenic actions of TRβY406F could be modulated by cellular context, we stably expressed TRβ1 (designated as TRβ), TRβ1PV (designated as PV), or TRβY406F in rat thyroid PCCL3 cells. PV is a TRβ mutant derived from a patient with resistance to thyroid hormone (RTH) [20]. Compelling evidence has shown that PV functions as an oncogene [16–18]. Figure 1A shows that the protein levels of TRβ (lane 2), PV (lane 3), and TRβY406F (lane 4) were similar as detected by a polyclonal antibody against the A/B domain of TRs. In contrast, only background was detected in the control cell line in which only the vector expressing the selector marker, neomycin (Neo) (lane 1). In addition, we also carried out reporter assays to confirm the functionality of the expressed proteins. For positive controls, when TRβ was exogenously transfected into the parental PCCL3 cells, T3-dependent transcriptional activation was detected (bar 2, Figure 1B). In contrast, when PV was exogenously transfected into the parental PCCL3, no T3-dependent

transcriptional activation was detected (bar 3). T3-dependent transcriptional activation was detected in cells stably expressing TRβ (PCCL3-TRβ cells) (bar 4), but not in cells stably expressing PV (PCCL3-PV cells) (bar 5). We have shown previously that Y406 mutation to F406 does not affect T3 binding of TRβ [15]. Consistent with these findings, Figure 1B shows that TRβY406F stably expressed in PCCL3 cells exhibited T3-dependent transcriptional activity (bar 6). These data indicate that TRβ and TRβY406F stably expressed in PCCL3 cells transcriptionally active and that PV had lost transcriptional activity as expected.

Previously we showed that breast cancer MDA cells stably expressing TRβY406F lost the tumor suppressor function of wild-type TRβ. To ascertain whether TRβY406F also lost the tumor suppressor function of wild-type TRβ in thyroid cells, we used the xenograft models. Athymic mice were fed with propylthiourea (PTU) to elevate thyroid-stimulating hormone (TSH), and PTU-treated mice were inoculated with PCCL3-TRβY406F cells. PCCL3-Neo cells and PCCL3-TRβ cells were similarly inoculated into PTU-treated mice as controls. Since we have shown that PV is an oncogene [16–18], we also inoculated PCCL3-PV cells into athymic mice for comparison. Figure 2A shows that PCCL3-Neo cells developed tumors, reaching the end point by 7 wk (closed circles). PCCL3-TRβY406F cells developed tumors after a brief lag time, but reached a slightly larger tumor size within 4 wk (closed diamonds; see also Figure 2B, bar4). PCCL3-PV cells, after a brief lag time, also developed tumors with the same size as that of PCCL3-Neo cells (closed triangles; see Figure 2B, bar 3). Remarkably, barely detectable tumors were found for PCCL3-TRβ cells after 13 wk (closed squares; Figure 1A and B, bar 2).

We next used immunohistochemical analysis to evaluate the proliferation activity of tumor cells with the use of the proliferation marker Ki67. As shown in Figure 2C, more and stronger Ki67 signals were detected in tumors derived from PCCL3-Neo cells (panels b and c), PCCL3-PV cells (panels h and i), and PCCL3-TRβY406F cells (panels k and l). In contrast, weaker and fewer Ki67 signals were found in tumors derived from PCCL3-TRβ cells (panels e and f). The quantitative data from counting the positively stained cells indicate clearly that fewer proliferating cells (a 40% lower number) were found in the tumor cells derived from PCCL3-TRβ (bar 2, Figure 2D) than in tumors derived from PCCL3-Neo cells (bar 1), PCCL3-PV cells (bar 3), and PCCL3-TRβY406F cells (bar 4, Figure 2D). In Figure 2C, panels a, d, g, and j are the negative controls in which only IgG was used. Taken together, these results clearly show that TRβ acted as a tumor suppressor to inhibit tumor growth, whereas PV and TRβY406F had lost the tumor suppressor functions.

To understand the molecular basis of the different levels of proliferation activity found in cells in the four tumors, we evaluated the activation of cSrc and key cell cylcie regulators. Previously we showed that in breast cancer cell lines, TRβY406F activated cSrc activity [15]. We therefore, determined whether cSrc activity was elevated by TRβY406F in PCCL3 cells. Figure 3 shows that the protein abundance of p-cSrc was higher in PCCL3-TRβY406F cells (panel a: lanes 7 and 8; see also quantitative data in data in Figure 3B-a, bar 4) and in PCCL3-PV cells (panel a: lanes 5 and 6; see also quantitative data in Figure 3B-a, bar 3) than in PCCL3-TRβ tumor cells (lanes 3 and 4; also in Figure 3B-a, bar 2). We also found that the protein abundance of cyclin D1 was lower in PCCL3-TRβ tumor cells (Figure 3A,

panel c: lanes 3 and 4; see also quantitative data in Figure 3B-b, bar 2) than in PCCL3-Neo, PCCL3-PV, and PCCL3-TRβY406F tumor cells (panel b: lanes 1 and 2; lanes 5 and 6; and lanes 7 and 8; see also bars 1, 3, and 4 in Figure 3B-b). The higher cyclin D1 led to an increase in phosphorylated retinoblastoma protein (p-Rb S780) in PCCL3-Neo, PCCL3-PV, and PCCL3-TRβY406F tumor cells (panel d: lanes 1 and 2; lanes 5 and 6; and lanes 7 and 8; see also bars 1, 3, and 4 in Figure 3B-c). Increased phosphorylation of Rb leads to release of the associated-E2F from unphosphorylated Rb-E2F complexes to drive the expression of transcription factors, thereby propelling cells to enter the S-phase to increase cell proliferation [21]. Since vascular endothelial growth factor (VEGF) is critical in the growth of solid tumors because of the need for an adequate blood supply [22], we also compared the protein abundance of VEGF in the cells from the four tumors. We found that the protein abundance of VEGF was lowest in PCCL3-TRβ tumor cells (panel f: lanes 3 and 4; see also quantitative data in Figure 3B-d, bar 2) as compared with PCCL3-Neo, PCCL3-PV, and PCCL3-TRβY406 tumor cells (panel f: lanes 1, 2; lanes 5 and 6; and lanes 7 and 8; see also bars 1, 3, and 4 in Figure 3B-d). These results indicate that TRβ could act to inhibit cell proliferation by suppressing the expression of key cell cycle regulators and to impede tumor growth by lowering VEGF to decrease vasculogenesis.

Loss of the cSrc Phosphorylation Site at Y406 of TRβ Promotes Cell Survival to Increase Tumor Growth

To understand whether the oncogenic actions of PV and TRβY406F mutants caused distinct histopathological features, we examined the H&E-stained tumor sections (Figure 4A). At a higher magnification, we detected proliferating cells in the regions marked as viable tumor-growth areas in all four types of tumor cells. Interestingly, we also found prominent necrotic areas in tumors derived from PCCL3-Neo cells (panels a and b, Figure 4A) and PCCL3-PV cells (panels e and f). But only a few necrotic areas were found in the tumor derived from PCCL3-TRβ cells (panels c and d) and necrosis was barely discernable in the tumor derived from PCCL3-TRβY406F cells (panels g and h, Figure 4A). To quantify the frequency of occurrence of necrosis, we measured the area of each part of each section with viable tumor and that with necrosis at a low magnification (Figure 4B-I). Consistent with the larger size shown in Figure 2B, the cross section of TRβY406F-tumor (panels m–p) was clearly larger than that of PCCL3-Neo panels a–d), PCCL3-TRβ (panels e–h), and PCCL3-PV (panels i–l, Figure 4B; quantitative data shown in Figure 4B-II). Remarkably, we found that the percentage of necrotic area was high in the tumors derived from PCCL3-Neo cells and PCCL3-PV cells (18.3% and 29.2%, respectively; bars 1 and 3, Figure 4B-III), but was very low (1.2%) in tumors derived from PCCL3-TRβY406F cells (bar 3, Figure 4B-III). However, the tumor derived from PCCL3-TRβ cells was too small for accurate measurement of the necrotic areas. These results indicate that the tumors derived from PCCL3-Neo cells and PCCL3-PV cells were highly necrotic, but the tumor derived from PCCL3-TRβY406F was barely necrotic suggesting different oncogenic molecular pathways in tumorigenesis for PV and TRβY406F mutants.

The markedly low level of necrosis detected in tumors derived from PCCL3-TRβY406F cells prompted us to ascertain the underlying molecular events. Necrosis in histology implies areas of cell death in tissues that can be caused by processes of overt damage, such as

mechanical injury, deprivation of oxygen or blood supply, or chemical damage. At the cellular level, necrosis is evident by organelle damage, nuclear swelling, and lyzed cell membrane ingested by macrophages [23]. On the other hand, necrosis can have other paths, such as apoptosis that is mediated by expression of pro-apoptotic genes and their effectors, leading to mitochondrial damage, nuclear shrinkage, and cell membrane lysis as a terminal event [24,25]. It is possible that a necrotic area in a tumor is a mixture of both mechanisms, where apoptotic death of some cells leads to necrosis of nearby cells caused by the liberated cell debris and toxins, poor blood supply, and inflammation. We therefore, examined the protein level of tumor necrosis factor α (TNFα), a cell-signaling molecule involved in inflammation. Consistent with the smallest necrotic areas shown in Figure 4B-I, the protein level of TNFα in tumors derived from PCCL3-TRβY406F cells was lower than in tumors derived from PCCL3-Neo cells and PCCL3-PV cells (lanes 7–9 vs. 1–and 4–6, Figure 5A-I-a; also quantitative data in Figure 5A-II-a). We further used immunohistochemistry to determine the protein abundance of TNFα in the tumor cells. Consistent with the western blot analysis, less intensive and fewer TNFα signals were detected in tumors derived from PCCL3-TRβY406F cells (panels h and I, Figure 5A-III-a) than in tumors derived from PCCL3-Neo cells and PCCL3-PV cells (panels b and c; and e and f, Figure 5A-II-a; see quantitative data in Figure 5A-II-b). Panels a, d, and g (Figure 5A-III-a) show the negative controls from using IgG only.

We next evaluated the activity of the downstream effector, NFκB (nuclear factor kappa-light-chain-enhancer of activated B cells). NFκB is a transcription factor whose activity is regulated by IκBα (nuclear factor of kappa light polypeptide gene enhancer in B-cells inhibitor, alpha). IκBα inhibits NFκB by masking the nuclear localization signals of NFκB proteins and keeping them sequestered in an inactive state in the cytoplasm [26]. In addition, IκBα blocks the ability of NFκB transcription factors to bind to DNA, which is required for NFκB's transcriptional activity. However, phosphorylation of IκBα by IκB kinase (IKK) results in the degradation by the proteasome pathway such that IκBα is released from the NFκB protein complex to allow translation of NFκB to nuclease to act as a transcription factor [26]. Figure 5A-I-b shows that p-IκBα protein levels were lower than in tumors derived from PCCL3-TRβY406F cells than in tumors derived from PCCL3-Neo cells and PCCL3-PV cells (lanes 7–9 vs. 1–3 and 4–6, Figure 5A-I-b), while the total IκBα protein levels were not significantly changed (Figure 5A-I-c; also quantitative data in Figure 5A-II-b). These data suggested that the TNFα-IκBα-NFκB signaling was attenuated in tumors derived from PCCL3-TRβY406F cells, but not in tumors derived from PCCL3-Neo cells and PCCL3-PV cells. This attenuated signaling decreased necrotic activity and increased tumor growth.

Moreover, TNFα-IκBα-NFκB signaling is also known to regulate apoptosis by controlling the expression of pro-apoptotic key regulators. Figure 5A-I-d shows that the protein levels of pro-apoptotic BAX was lower in tumors derived from PCCL3-TRβY406F cells than in tumors derived from PCCL3-Neo and PCCL3-PV cells, (lanes 7–9, vs. lanes 1–6; also see quantitative data, Figure 5A-II-c). Consistently, we also found that the protein levels of cysteine-aspartic proteases (e.g., caspase 8) that play an essential role in apoptosis and necrosis [27,28] were lower in tumors derived from PCCL3-TRβY406F cells than in tumors derived from PCCL3-Neo and PCCL3-PV cells (panel e, lanes 7–9 vs. lanes 1–6; Figure 5A-

I-e; also see quantitative data, Figure 5A-II, panel d). These data indicate that the decreased apoptotic activity mediated by TRβY406F contributed to the growth in tumors derived from PCCL3-TRβY406F cells.

DISCUSSION

The notion that TRβ could function as a tumor suppressor derives from earlier observations that the loss of heterozygosity and/or truncating of the *THRB* gene is associated with human cancers. Subsequently, data from cell-based analyses and in vivo studies have provided many lines of evidence to support this notion. One piece of compelling evidence came from extensive studies of a mutant mouse expressing a dominant negative TRβ C-terminal frame-shift mutant, PV [16, 29], in that the loss of TR normal functions drives carcinogenesis of thyroid and promotes the aberrant growth of the pituitary [30] and the breast [31]. Other collaborative evidence came from the studies showing that ectopically over-expressed TRβ suppresses the cancer phenotypes [12,13]. Our previous studies have elucidated that phosphorylation of TRβ on Y406 by cSrc is critical in the tumor suppression of TRβ in breast cancer cells. The present studies have shown that the critical role of cSrc-induced phosphorylated Y406 in mediating the tumor suppressor functions of TRβ is not limited in breast cancer cells. PCCL3 cells are normal rat thyroid cells. In our preliminary studies, we found that in the absence of elevated TSH, no tumors were developed from PCCL3-Neo cells. We therefore, treated the athymic mice to elevate the TSH levels. Tumors were developed from the injected PCCL3-Neo cells. That tumors were developed from the injected PCCL3 cells in mice with elevated TSH are consistent with accumulated evidence to indicate that high TSH concentrations are closely associated with an increased risk of thyroid cancer [32–35]. Thus, PCCL3 cells xenograft tumors could serve as a model to reflect the effects of TSH on follicular cell tumorigenesis. Remarkably, tumors were barely detectable in athymic mice inoculated with PCCL3-TRβ cells in spite of elevated TSH levels, indicating a strong tumor suppressing activity by TRβ. In PCCL3-TRβY406F cells, not only was the suppressor activity of wild-type TRβ lost, but also the induced tumors were larger than those induced by control PCCL3-Neo cells (see Figure 2B). These results indicate that the critical role of Y406 phosphorylation by cSrc in the tumor suppressing function of TRβ is not limited to breast cancer cells, but could be extended to thyroid cells. Additional work further examining the role of Y406 phosphorylation in other cell types could establish that this is a general molecular mechanism applicable in all cell types that accounts for the tumor suppressor function of TRβ.

In the present studies, we discovered that while mutations of PV and Y406F abolished the tumor suppressor functions of TRβ, the resulting oncogenic phenotypic manifestations of PV and TRβ Y406F differed. Tumors derived from TRβY406F cells developed faster and became larger than tumors derived from PV cells (see Figure 2A and B). Tumors derived from TRβY406F cells exhibited less necrosis than tumors derived from PV cells (Figure 4). Molecular analysis showed that TRβY406F, but not PV, attenuated the TNFα-IκBα-NFkB signaling, thus lowering necrotic activity and apoptosis and further promoting tumor cell proliferation. The different oncogenic actions between PV and TRβY406F could be anticipated as these two mutants have different molecular characteristics. PV has a frame-shift mutation at the C-terminal 14 amino acids [20], resulting in the total loss of T3 binding

activity and transcription capacity. In our in vivo studies using the *Thrb*^{PV} mouse, we have elucidated that the oncogenic actions could be initiated at the transcription levels as well as through extra-nuclear actions [16]. In contrast, TRβY406F retained its T3 binding activity and transcription capacity [15]. Its oncogenic actions are mainly via phosphorylation cascades. Thus, the oncogenic actions of TRβ mutants depend on the sites of mutations and the functional characteristics of the mutants. This notion would suggest that potential oncogenic mutations of the *THRB* gene could lead to different cancer phenotypes.

The role of TSH in thyroid carcinogenesis has been debated for years. Some studies have implied that TSH could act to initiate thyroid carcinogenesis [36,37], and suggested that high TSH concentrations are closely associated with an increased risk of thyroid cancer [32–35]. However, other reports have disputed this possibility [38–40]. Previously, we crossed the *Thrb*$^{PV/PV}$ mouse, a model of follicular thyroid cancer, with mice deficient in the TSH receptor gene (TSHR$^{-/-}$ mice). Analysis of phenotypes of the offspring from the cross of these two mutant mice indicated that thyroid growth stimulated by TSH is a prerequisite but is not sufficient for metastatic cancer to occur. Additional genetic alterations, destined to alter focal adhesion and migration capacities, are required to empower hyperplastic follicular cells to invade and metastasize [41]. In line with these findings, we found that the athymic mice without elevated TSH by PTU treatment that were inoculated with PCCL3-Neo cells failed to develop tumors. These findings suggested that in athymic mice, TSH is necessary prerequisite to stimulate cell proliferation. Also, the lack of proper immune surveillance in athymic mice facilitated tumorigenesis even without oncogenic mutations in PCCL3-Neo cells. In PCCL3-TRβ cells, the tumor suppress or function of TRβ blocked tumor development in spite of the athymic mice's lack of proper immune surveillance. However, the mutations such as TRβY406F or PV led to the loss of tumor suppressor functions of TRβ in mice with elevated TSH. These observations would suggest that elevated TSH could potentially be a risk factor in thyroid cancer susceptibility in a subpopulation of patients with compromised immunity.

Acknowledgments

Grant sponsor: Intramural Research Program at the Center for Cancer Research; Grant sponsor: National Cancer Institute; Grant sponsor: National Institutes of Health

REFERENCES

1. Weinberger C, Thompson CC, Ong ES, Lebo R, Gruol DJ, Evans RM. The c-erb-A gene encodes a thyroid hormone receptor. Nature 1986;324:641–646. [PubMed: 2879243]
2. Leduc F, Brauch H, Hajj C, et al. Loss of heterozygosity in a gene coding for a thyroid hormone receptor in lung cancers. Am J Hum Genet 1989;44:282–287. [PubMed: 2536219]
3. Sisley K, Cottam DW, Rennie IG, et al. Non-random abnormalities of chromosomes 3, 6, and 8 associated with posterior uveal melanoma. Genes Chromosomes Cancer 1992;5:197–200. [PubMed: 1384670]
4. Chen LC, Matsumura K, Deng G, et al. Deletion of two separate regions on chromosome 3p in breast cancers. Cancer Res 1994;54:3021–3024. [PubMed: 7910519]
5. Gonzalez-Sancho JM, Garcia V, Bonilla F, Munoz A. Thyroid hormone receptors/THR genes in human cancer. Cancer Lett 2003;192:121–132. [PubMed: 12668276]

6. Joseph B, Ji M, Liu D, Hou P, Xing M. Lack of mutations in the thyroid hormone receptor (TR) alpha and beta genes but frequent hypermethylation of the TRbeta gene in differentiated thyroid tumors. J Clin Endocrinol Metab 2007;92: 4766–4770. [PubMed: 17911173]
7. Ling Y, Xu X, Hao J, et al. Aberrant methylation of the THRB gene in tissue and plasma of breast cancer patients. Cancer Genet Cytogenet 2010;196:140–145. [PubMed: 20082849]
8. Iwasaki Y, Sunaga N, Tomizawa Y, et al. Epigenetic inactivation of the thyroid hormone receptor beta1 gene at 3p24.2 in lung cancer. Ann Surg Oncol 2010;17:2222–2228. [PubMed: 20155399]
9. Li Z, Meng ZH, Chandrasekaran R, et al. Biallelic inactivation of the thyroid hormone receptor beta1 gene in early stage breast cancer. Cancer Res 2002;62:1939–1943. [PubMed: 11929806]
10. Martinez-Iglesias O, Garcia-Silva S, Tenbaum SP, et al. Thyroid hormone receptor beta1 acts as a potent suppressor of tumor invasiveness and metastasis. Cancer Res 2009;69:501–509. [PubMed: 19147563]
11. Garcia-Silva S, Aranda A. The thyroid hormone receptor is a suppressor of ras-mediated transcription, proliferation, and transformation. Mol Cell Biol 2004;24:7514–7523. [PubMed: 15314161]
12. Kim WG, Zhao L, Kim DW, Willingham MC, Cheng SY. Inhibition of tumorigenesis by the thyroid hormone receptor beta in xenograft models. Thyroid 2014;24: 260–269. [PubMed: 23731250]
13. Park JW, Zhao L, Cheng SY. Inhibition of estrogen-dependent tumorigenesis by the thyroid hormone receptor beta in xenograft models. Am J Cancer Res 2013;3:302–311. [PubMed: 23841029]
14. Martinez-Iglesias OA, Alonso-Merino E, Gomez-Rey S, et al. Autoregulatory loop of nuclear corepressor 1 expression controls invasion, tumor growth, and metastasis. Proc Natl Acad Sci USA 2016;113:E328–E337. [PubMed: 26729869]
15. Park JW, Zhao L, Webb P, Cheng SY. Src-dependent phosphorylation at Y406 on the thyroid hormone receptor beta confers the tumor suppressor activity. Oncotarget 2014; 20:10002–10016.
16. Guigon CJ, Cheng SY. Novel oncogenic actions of TRbeta mutants in tumorigenesis. IUBMB Life 2009;61:528–536. [PubMed: 19391168]
17. Guigon CJ, Cheng SY. Novel non-genomic signaling of thyroid hormone receptors in thyroid carcinogenesis. Mol Cell Endocrinol 2009;308:63–69. [PubMed: 19549593]
18. Park JW, Zhao L, Willingham M, Cheng SY. Oncogenic mutations of thyroid hormone receptor beta. Oncotarget 2015;6:8115–8131. [PubMed: 25924236]
19. Guigon CJ, Zhao L, Willingham MC, Cheng SY. PTEN deficiency accelerates tumour progression in a mouse model of thyroid cancer. Oncogene 2009;28:509–517. [PubMed: 18997818]
20. Parrilla R, Mixson AJ, McPherson JA, McClaskey JH, Weintraub BD. Characterization of seven novel mutations of the c-erbA beta gene in unrelated kindreds with generalized thyroid hormone resistance. Evidence for two “hot spot” regions of the ligand binding domain. J Clin Invest 1991;88:2123–2130. [PubMed: 1661299]
21. Coller HA. What’s taking so long? S-phase entry from quiescence versus proliferation. Nat Rev Mol Cell Biol 2007;8:667–670. [PubMed: 17637736]
22. Goel HL, Mercurio AM. VEGF targets the tumour cell. Nat Rev Cancer 2013;13:871–882. [PubMed: 24263190]
23. Balkwill F Tumour necrosis factor and cancer. Nat Rev Cancer 2009;9:361–371. [PubMed: 19343034]
24. Proskuryakov SY, Konoplyannikov AG, Gabai VL. Necrosis: A specific form of programmed cell death? Exp Cell Res 2003;283:1–16. [PubMed: 12565815]
25. Edinger AL, Thompson CB. Death by design: Apoptosis, necrosis and autophagy. Curr Opin Cell Biol 2004;16: 663–669. [PubMed: 15530778]
26. Oeckinghaus A, Hayden MS, Ghosh S. Crosstalk in NF-kappaB signaling pathways. Nat Immunol 2011;12:695–708. [PubMed: 21772278]
27. Han J, Zhong CQ, Zhang DW. Programmed necrosis: Backup to and competitor with apoptosis in the immune system. Nat Immunol 2011;12:1143–1149. [PubMed: 22089220]

28. Mocarski ES, Upton JW, Kaiser WJ. Viral infection and the evolution of caspase 8-regulated apoptotic and necrotic death pathways. Nat Rev Immunol 2012;12:79–88.
29. Suzuki H, Willingham MC, Cheng SY. Mice with a mutation in the thyroid hormone receptor beta gene spontaneously develop thyroid carcinoma: A mouse model of thyroid carcinogenesis. Thyroid 2002;12:963–969. [PubMed: 12490073]
30. Furumoto H, Ying H, Chandramouli GV, et al. An unliganded thyroid hormone beta receptor activates the cyclin D1/cyclin-dependent kinase/retinoblastoma/E2F pathway and induces pituitary tumorigenesis. Mol Cell Biol 2005;25:124–135. [PubMed: 15601836]
31. Guigon CJ, Kim DW, Willingham MC, Cheng SY. Mutation of thyroid hormone receptor-beta in mice predisposes to the development of mammary tumors. Oncogene 2011;30: 3381–3390. [PubMed: 21399657]
32. Ozemir IA, Gurbuz B, Bayraktar B, et al. The effect of thyroid-stimulating hormone on tumor size in differentiated thyroid carcinoma. Indian J Surg 2015;77:967–970. [PubMed: 27011492]
33. Zheng J, Li C, Lu W, Wang C, Ai Z. Quantitative assessment of preoperative serum thyrotropin level and thyroid cancer. Oncotarget 2016;23:34918–34929.
34. Fighera TM, Perez CL, Faris N, et al. TSH levels are associated with increased risk of thyroid carcinoma in patients with nodular disease. Endokrynol Pol 2015;66:480–485. [PubMed: 26662646]
35. Shi RL, Liao T, Qu N, Liang F, Chen JY, Ji QH. The usefulness of preoperative thyroid-stimulating hormone for predicting differentiated thyroid microcarcinoma. Otolaryngol Head Neck Surg 2016;154:256–262. [PubMed: 26598500]
36. Fiore E, Vitti P. Serum TSH and risk of papillary thyroid cancer in nodular thyroid disease. J Clin Endocrinol Metab 2012;97: 1134–1145. [PubMed: 22278420]
37. Xing M Molecular pathogenesis and mechanisms of thyroid cancer. Nat Rev Cancer 2013;13:184–199. [PubMed: 23429735]
38. Tanaka K, Inoue H, Miki H, et al. Relationship between prognostic score and thyrotropin receptor (TSH-R) in papillary thyroid carcinoma: Immunohistochemical detection of TSH-R. Br J Cancer 1997;76:594–599. [PubMed: 9303357]
39. Matsumoto H, Sakamoto A, Fujiwara M, et al. Decreased expression of the thyroid-stimulating hormone receptor in poorly-differentiated carcinoma of the thyroid. Oncol Rep 2008;19:1405–1411. [PubMed: 18497944]
40. Davis PJ, Hercbergs A, Luidens MK, Lin HY. Recurrence of differentiated thyroid carcinoma during full TSH suppression: Is the tumor now thyroid hormone dependent? Horm Cancer 2015;6:7–12. [PubMed: 25292307]
41. Lu C, Zhao L, Ying H, Willingham MC, Cheng SY. Growth activation alone is not sufficient to cause metastatic thyroid cancer in a mouse model of follicular thyroid carcinoma. Endocrinology 2010;151:1929–1939. [PubMed: 20133453]

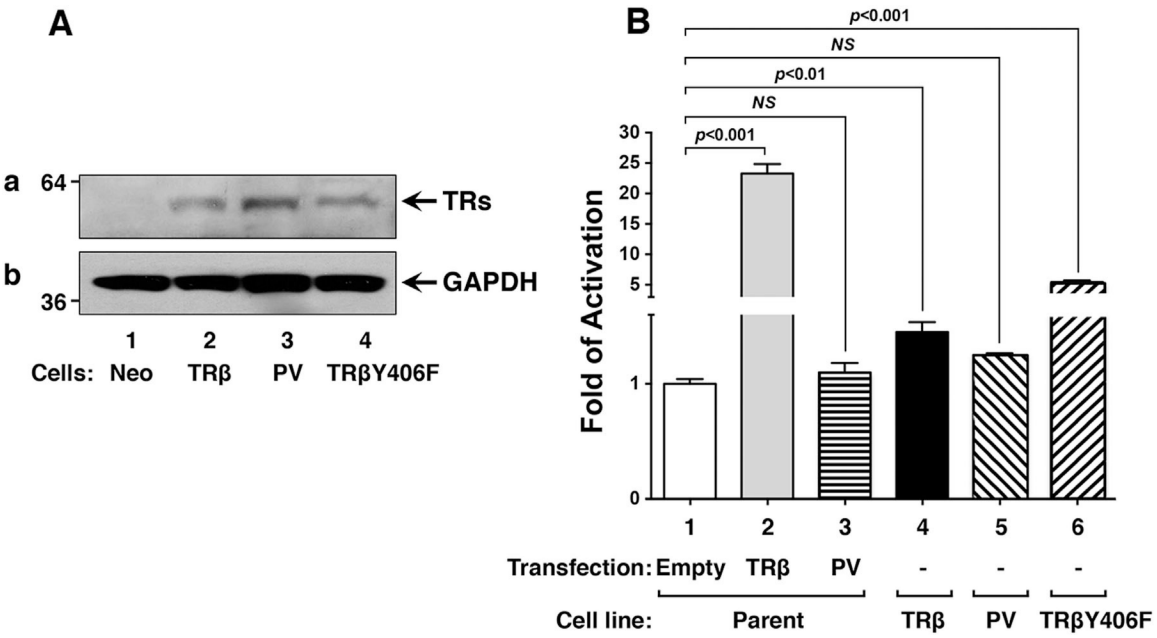

Figure 1.

Establishment of cell lines stably expressing TRβ, PV, and TRβY406F in PCCL3 cells. (A) TRβ, PV, and TRβY406F were similarly expressed in PCCL3 cells (lanes 2–4), but not in control PCCL3 cells (Neo, lane 1). Western blot analysis was carried out as described in Materials and Methods. (B) Reporter assays of the transiently expressed TRβ or PV in PCCL3 parental cell and stably expressed in cells (PCCl3-TRβ, PCCl3-PV, and PCCl3-TRβY406F) using a Pal-luc reporter construct. Results are presented as the relative fold luciferase activity of cells treated with T3 for 24 h compared with cells without T3 treatment (Td medium), reporter assay was carried out as described in Materials and Methods. *P*-values are as indicated.

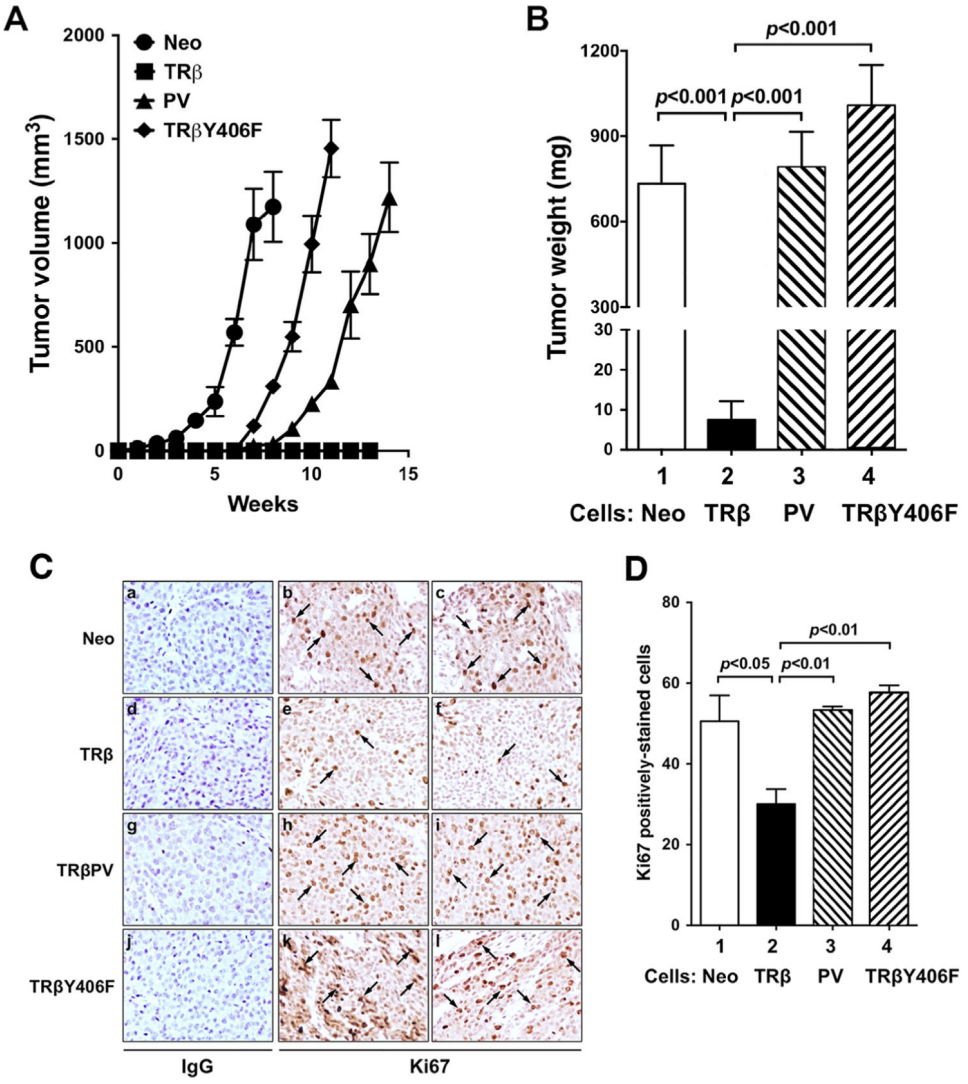

Figure 2.

Comparison of tumor growth characteristics of PCCl3-TRβ, PCCl3-PV, PCCl3-TRβY406F, and PCCL3-Neo control cells. (A) Tumor growth rates: Equal numbers of cells for four cell lines were inoculated onto the right flank of 6-wk-old female athymic NCr-nu/nu mice. Tumor sizes were measured weekly until reaching the end points and the rates of tumor growth were compared. (B) Tumors were dissected at the endpoint and the weight was determined. The data are expressed as mean ± SE ($n = 6$). (C) Immunohistochemical analysis using the Ki67 marker in tumor cells. Sections of tumors derived from Neo control cells (panels a–c), PCCl3-TRβ cells (panels d–f), PCCl3-PV cells (panels g–i), and PCCl3-TRβY406F cells (panels j–l) were treated with control IgG (panels a, d, g, and j) or with anti Ki67 antibodies (panels b and c, e and f, h and I, and k and l), as described in Materials and Methods. Ki67 positively stained cells are indicated by arrows. (D) Quantitative analysis of the Ki67 positively stained cells in the tumors derived from the four cell lines. The Ki-67-positive cells were counted from three different sections and expressed as percentage of Ki-67-positive cells versus total cells examined. The data are expressed as mean ± SEM ($n = 4$). The *P*-values are shown.

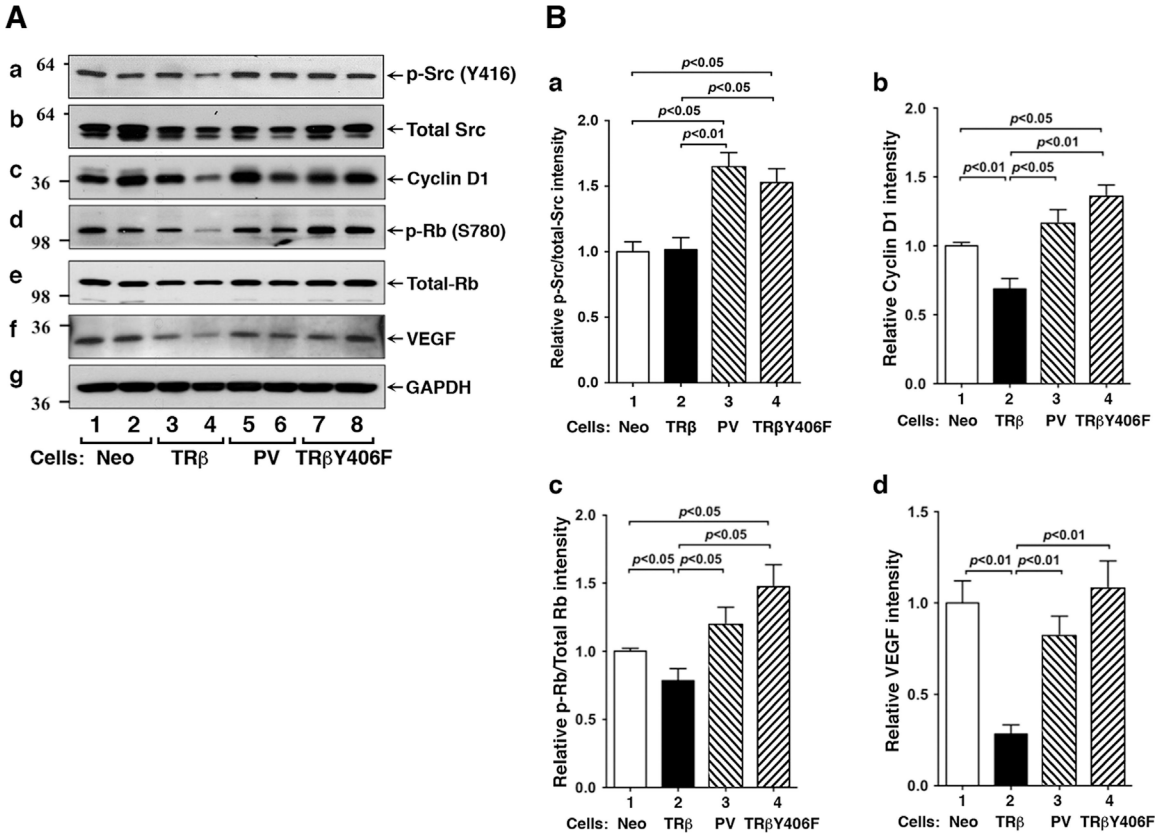

Figure 3.

Analysis of protein levels of cell proliferation regulators in tumors derived from Neo control cells, PCCL3-TRβ1, PCCL3-TRβ1PV, and PCCL3-TRβ1Y406F cells. (A) Western blot analysis of key regulators, cyclin D1 (panel a), p-Rb (panels b), total Rb (panel c), and VEGF (panel d) in tumors derived from PCCL3-Neo (lanes 1 and 2), PCCL3-TRβ (lanes 3 and 4), PCCL3-PV (lanes 5 and 6), and PCCL3-TRβY406F (lanes 7 and 8) cells. Tumors were excised from the injection sites (hind flanks) of athymic nude mice, and the Western blot analysis was carried as described in Materials and Methods. (B) The band intensities of the proteins detected in A were quantified and compared. The data are shown as mean ± SE ($n = 2$).

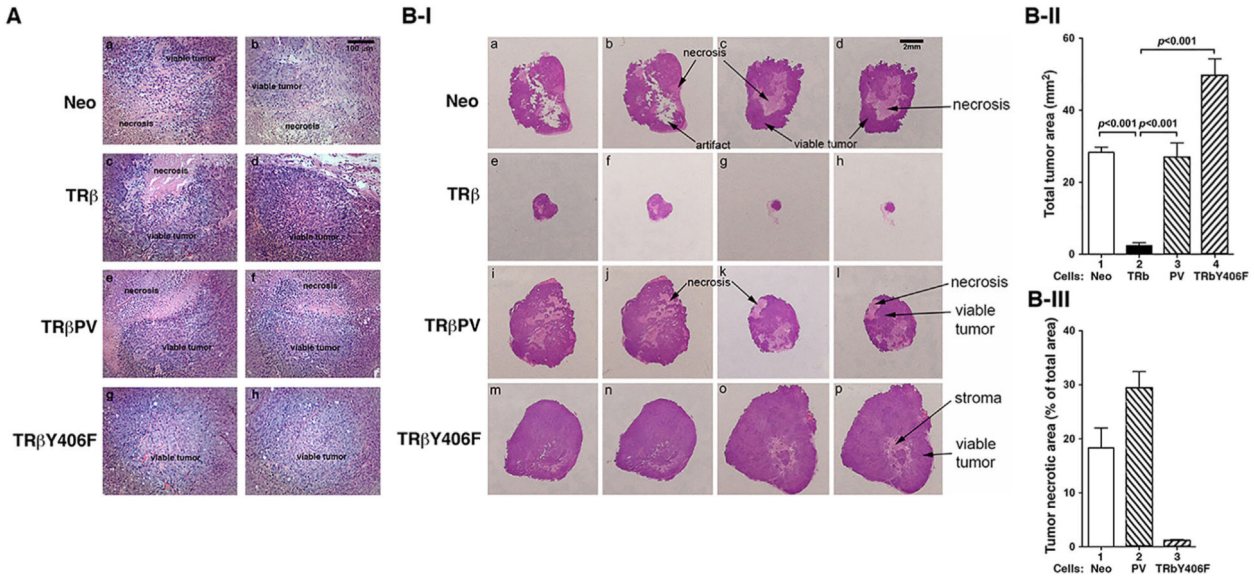

Figure 4.

Comparison of viable tumor growth area and tumor necrotic area of tumors derived from PCCL3-Neo (control), PCCL3-TRβ, PCCL3-PV, and PCCL3-TRβY406F cells. (A) Representative histological features of hematoxylin and eosin (H&E) stained sections of tumors derived from PCCL3-Neo (panels a and b), PCCL3-TRβ (panels c and d), PCCL3-PV (panels e and f), and PCCL3-TRβY406F (panels g and h) cells. (B) Representative necrotic area images of tumors derived from PCCL3-Neo (panels a and b), PCCL3-TRβ (panels c and d), PCCL3-PV (panels e and f), and PCCL3-TRβY406F (panels g and h) cells. (C) Quantitative image analysis of the total tumor areas from tumors derived from PCCL3-Neo, PCCL3-TRβ, PCCL3-PV, and PCCL3-TRβY406F cells, respectively. The *P*-values are shown. (D) Quantitative analysis of necrotic area as percentage of total tumor area for the tumors derived from PCCL3-Neo, PCCL3-PV, and PCCL3-TRβY406F cells. No quantitative data could be determined accurately because of the small size of the tumors derived from PCCL3-TRβ cells. The *P*-values are shown.

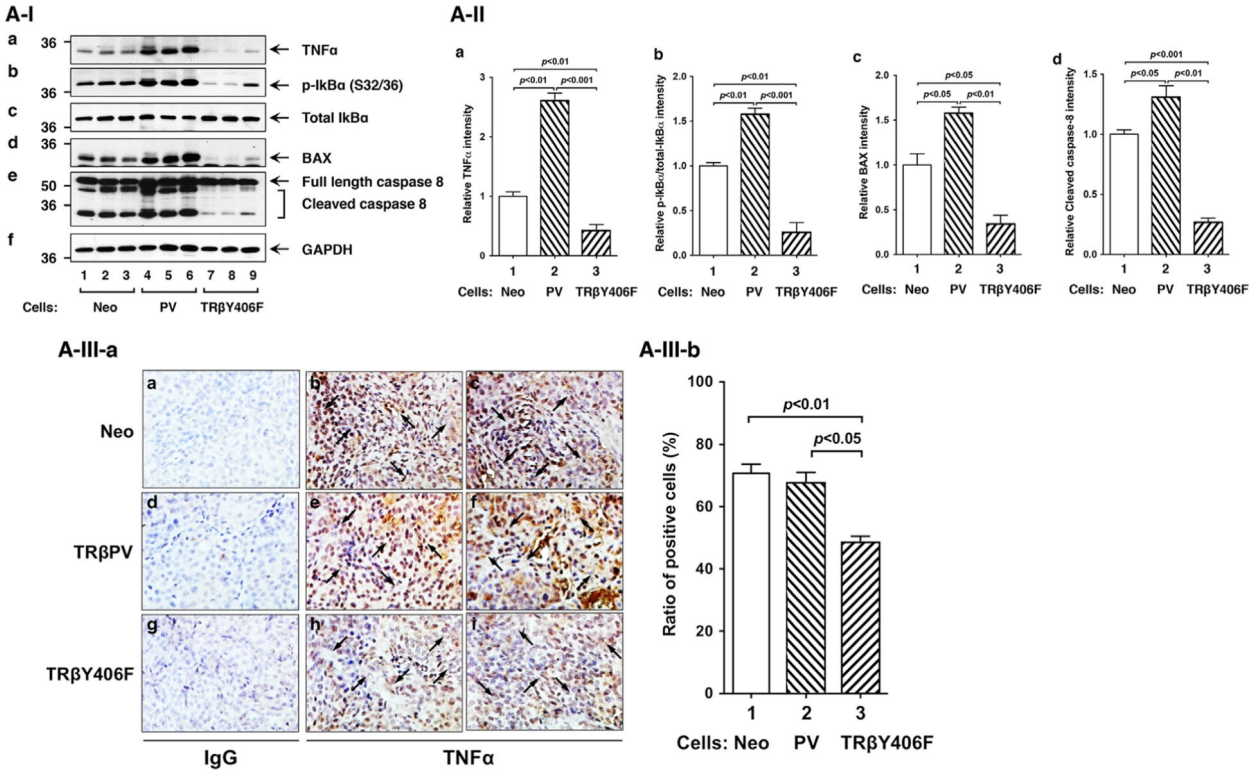

Figure 5.

Analysis of protein levels of necrosis regulators in tumors derived from PCCL3-Neo (control), PCCL3-PV, and PCCL3-TRβY406F cells. (A-I-a) Western blot analysis of TNF-α (panel a) and IκBα (panel b and c) and caspase-8 in tumors. Tumors were excised from the injection sites (hind flanks) of athymic nude mice, and Western blot analysis was carried out as described in Materials and Methods. (A-I-b) The band intensities of the protein detected in A-I-a were quantified and compared. The data are shown as mean ± SE ($n = 2$). (A-II-a) Immunohistochemical analysis of TNFα in tumors from PCCL3-Neo (control), PCCL3-PV, and PCCL3-TRβY406F cells. Sections of tumors derived from PCCL3-Neo control cells (panels a–c), PCCl3-TRβPV cells (panels d–f), and PCCl3-TRβY406F cells (panels g–i) were treated with control anti-IgG (panels a, d, g) or with anti-TNFα antibodies (panels b, c, e, f, h, and i) as described in Materials and Methods. The TNFα positively stained cells are indicated by arrows. (A-II-b) The TNFα-positive cells were counted from three different sections and expressed as percentage of TNFα-positive cells versus total cells examined. The data are expressed as mean ± SEM ($n = 4$). The *P*-values are shown.